RESEARCH PAPER

Flexural behaviour of structural fibre composite sandwich beams in flatwise and edgewise positions

(Title contains 13 words)

Running headline: Flexural behaviour of structural composite sandwich beams in flatwise and edgewise positions (81 characters)

by

Allan Manalo, Thiru Aravinthan, Warna Karunasena and **Mainul Islam**
Centre of Excellence in Engineered Fibre Composites (CEEFC),
Faculty of Engineering and Surveying, University of Southern Queensland,
Toowoomba, Queensland 4350, Australia

Submitted to
Composite Structures

Corresponding Author:

Thiru Aravinthan
Associate Professor
Centre of Excellence in Engineered Fibre Composites (CEEFC),
Faculty of Engineering and Surveying, University of Southern Queensland,
Toowoomba, Queensland 4350, Australia
Tel: +61 7 4631 1385 Fax: +61 7 4631 2110
E-mail: aravinthant@usq.edu.au

Manuscript summary:

Total pages	22 (including 1-page cover)
Number of figures	17
Number of tables	4

Flexural behaviour of structural fibre composite sandwich beams in flatwise and edgewise positions

A.C. Manalo, T. Aravinthan*, W. Karunasena, M.M. Islam

Centre of Excellence in Engineered Fibre Composites (CEEFC), University of Southern Queensland, Toowoomba 4350, Australia

Abstract

The flexural behaviour of a new generation composite sandwich beams made up of glass fibre reinforced polymer skins and modified phenolic core material was investigated. The composite sandwich beams were subjected to 4-point static bending test to determine their strength and failure mechanisms in the flatwise and the edgewise positions. The results of the experimental investigation showed that the composite sandwich beams tested in the edgewise position failed at a higher load with less deflection compared to specimens tested in the flatwise position. Under flexural loading, the composite sandwich beams in the edgewise position failed due to progressive failure of the skin while failure in the flatwise position is in a brittle manner due to either shear failure of the core or compressive failure of the skin followed by debonding between the skin and the core. The results of the analytical predictions and numerical simulations are in good agreement with the experimental results.

Keywords: Structural composite sandwich beams; Fibre composites; Modified phenolic core; Flexure; Flatwise; Edgewise.

*Corresponding author, tel. +61 7 4631 1385; fax. +61 7 4631 2110
E-mail addresses: manalo@usq.edu.au (A.C. Manalo), aravinthant@usq.edu.au (T. Aravinthan), karunasa@usq.edu.au (W. Karunasena), islamm@usq.edu.au (M.M. Islam)

1. Introduction

A structural sandwich is a special form of a laminated composite fabricated by attaching two thin but stiff skins to the lightweight but thick core [1]. The main benefit of using the sandwich concept in structural components is its high bending stiffness and high strength to weight ratios [2]. In addition, sandwich constructions are preferred over conventional materials because of its high corrosion resistance [3]. With its many advantages, composite sandwich structures have been widely used in the automotive, aerospace, marine and other industrial applications. This composite material also draws a lot of interest in the construction industry and is now beginning to be in use for civil engineering applications [4].

Recent applications have demonstrated that fibre composite sandwich construction can be effectively and economically used in the civil infrastructure. An innovative hybrid box section consisting of GFRP pultruded box with an upper layer of concrete in the compression side is proposed by Canning et al. [5]. The web of the beam section is made up of sandwich construction to prevent buckling. A monocoque fibre composite truss concept which uses two planner skins that contain the fibre separated by a core material was designed and developed by Humpreys et al. [6]. Another is the deployable shelter using modular fibre composite truss panel as the main structural system [7]. The diagonal members of the truss are made of composite sandwich structure. An Advanced Composite Construction System (ACCS) made from pultruded fibre-reinforced polymer composite with polyethylene foam core was developed for use in walls and floors of a two-storey building structure [8]. Other structures constructed using composite sandwich profiles are highway bridge deck systems [9] and temporary bypass roadways [10].

The many advantages of fibre composite sandwich structure favour its application for civil infrastructure. However, very limited attempt has been made so far to use these materials for structural beam application although engineers have a wide range of composite sandwich panels. The main reason could be that most of the currently used core materials are not appropriate for

this type of structural application. Normally, the core material is made of low strength foam material, but its thickness provides the sandwich composite with high bending stiffness with overall low density [11]. These types of composite sandwich structure are sensitive to failure by the application of compressive loads [12]. On the other hand, composite sandwich panels with honeycomb or open-cell lattice truss structure core are highly efficient from a weight standpoint and have good compression performance [13]. However, the cavities between the skins of honeycomb and truss cores reduce the capacity of these composite sandwich materials to hold mechanical connectors. Furthermore, it has been demonstrated that during flexural loading, most sandwich construction failed due to shear failure of the core [14, 15]. The evolution of composite sandwich structure with high strength but lightweight core material could be an emerging alternative construction material for structural elements.

Recently, a new generation fibre composite sandwich panel has been developed in Australia [16]. The satisfactory performance in several building and residential projects and the flexibility of this innovative composite sandwich panel has shown a high possibility in using this material in the development of structural beams. As these composite sandwich panels are produced in limited thicknesses, a structural beam section from this material could be attained by gluing a number of sandwich panels either in the flatwise (horizontal) and the edgewise (vertical) positions or combinations of both. This concept is similar to laminated veneer lumber used in timber engineering where several smaller pieces of wood are horizontally or vertically laminated (either by nailing or gluing) to produce a single large structural member to support a greater load. Furthermore, this concept is anticipated to lead towards the improvement of structural performance of composite sandwich structures while maintaining the simplicity of the production process. A detailed understanding of the behaviour and failure mechanisms of individual composite sandwich beams in the two different positions is therefore necessary to design a structure made from this composite material.

A number of researches have studied the behaviour and failure modes of sandwich structures in flexure [2, 11, 12, 17-19]. In these studies, sandwich specimens are tested in the flatwise position as it is commonly used as structural panels for roof, floor, walls and bridge decks. The skins located at the top and bottom carry the flexural load and the inner core, the shear. In beams and similar applications, structural components are used in the edgewise orientation for higher strength and stiffness. These applications are similar to structural plywood loaded in the plane of the panel when utilised as shear webs of composite box beams, I-beams or glue-laminated beams. Clearly, there is an application for such composite sandwich structure in the edgewise position. Currently, there are no available reports on the strength and failure mechanisms of sandwich beams tested in the edgewise position. Hence, the behaviour of composite sandwich beams under edgewise loading remains to be investigated as it may behave differently because the skins and the core are positioned to carry both flexure and shear.

In this paper, the flexural behaviour of a structural composite sandwich beams made up of phenolic core material and glass fibre composite skins is reported. The load-deflection behaviour, stress-strain behaviour, failure load and the failure mechanisms of this composite sandwich beams were evaluated under 4-point static bending in the flatwise and edgewise positions. The strength and stiffness of the composite sandwich beams were predicted theoretically using the properties of the skin and core materials established from the coupon tests and were compared with the experimental results. Finite element simulations were also conducted to further verify the strength and behaviour of the composite sandwich beams using the effective mechanical properties of the constituent materials.

2. Experimental program

2.1 Material properties

The structural composite sandwich beams tested in this study are made up of glass fibre composite skins co-cured onto the modified phenolic core material using a toughened phenol

formaldehyde resin [16]. The fibre composite skin is made up of 2 plies of stitched bi-axial E-CR glass fibres with $[0/90]_s$ stacking sequence (manufactured by Fiberex) and has a total thickness of around 1.8 mm. The modified phenolic foam core is a proprietary formulation by LOC Composites, Pty., Ltd, Australia. The composite sandwich beam has an overall density of around 990 kg/m^3 while the modified phenolic core has a density of 850 kg/m^3. The higher density of the core improved the compressive strength and rigidity of the composite sandwich structure. It will not crush easily under point loading and could be suitable for use in structural applications. Overall, the density of the composite sandwich beam is comparable to that of hardwood red gum timber which weighs 900 kg/m^3 air dried [20] but still very much less compared to concrete and steel which weigh 2,400 kg/m^3 and 7,850 kg/m^3 respectively.

Characterisation of the mechanical properties of the fibre composite skin and the modified phenolic core material has been performed using flexure, tensile, compressive and shear tests following the ISO and ASTM standards. The test specimen for the skin is manufactured by hand lay-up while the test specimen for the core material was obtained directly from the composite sandwich panels by sanding off the skins on both sides. Tables 1 and 2 summarise the effective mechanical properties of the skin and the core material determined from coupon test.

2.2 *Test specimen*

Composite sandwiches with nominal thicknesses of 18 mm and 20 mm were tested in this study. The composite sandwiches were cut into required specimen dimensions and tested without any treatment or modification. Five replicates for each specimen type were prepared and tested. The details of the specimen are listed in Table 3.

2.3 Test set-up and procedure

The static flexural test of composite sandwich beams was performed in accordance with the ASTM C393-00 standard [21]. For specimen 4FSW-I, the load was applied at the third and at the two-third points of the span (Figure 1a) while the load was applied at 0.4 and at 0.6 of the span for specimen 4FSW-II (Figure 1b) through a 100 kN servo-hydraulic universal testing machine with a loading rate of 3 mm/min. The loading pins and the supports had a diameter of 10 mm to prevent local indentation failure on the composite sandwich. For composite sandwiches tested in the edgewise position, steel plates were provided under the loading points to prevent premature failures. Figure 2 shows the actual test set-up and instrumentation for the static flexural test of composite sandwich beams. Strain gages were attached to the top and the bottom surfaces of the composite sandwich to evaluate the strain during loading and until final failure. The applied load, displacement and strains were recorded and obtained using a data logger.

3. Evaluation of composite sandwiches behaviour

Theoretical predictions of the failure load, stress-strain relationship and load-deflection behaviour of the composite sandwiches under flexural loads using the mechanical properties of the fibre composite skin and the core material established from coupon testing were conducted.

3.1 Estimation of failure loads and mechanisms

The failure mode of the composite sandwiches is determined by the geometry, material properties and the loading configuration. Figure 3 shows the different components of the composite sandwich section.

where: t = thickness of the skin

c = thickness of the core

b = width of the composite sandwich

h = total thickness of the sandwich, c+2t

d = distance between the centre of the skins, c+t.

The following are the most common failure mechanisms in composite sandwiches under bending [3, 22, 23].

a. skin compressive/tensile failure;
b. core shear failure; and
c. core failure in tension/compression

3.1.1 Skin failure (compression or tension)

Compression or tensile failure of the skin occurs when the axial stress in the sandwich face attains the maximum strength of the skin material. For a symmetrical composite sandwich, the peak strength, P_{sf} for this failure mode under four point bending can be predicted by:

$$P_{sf} = \frac{D\sigma_s}{CLE_s x} \qquad (1)$$

where: C = 1/6 for specimen 4FSW-I and 1/5 for specimen 4FSW-II

D = flexural stiffness

σ_s = maximum strength of skin

L = support span

E_s = modulus of elasticity of the skin

x = distance of the outermost layer of skin to centre of the composite sandwich

= (h/2) for flatwise position

= (b/2) for edgewise position

In the analysis of sandwich structures it is usually assumed that the core only supports the shear and the skins carry the tensile and compressive loads under flexure [24]. In the composite sandwich beams tested in this study, the contribution of the core and the skin in both flexural and

shear stiffness were considered. The flexural stiffness, *D* or *EI* of the sandwich beams in the flatwise direction is calculated using equation 2 and in the edgewise direction using equation 3.

$$EI_{(flat)} = \frac{bt^3}{6}E_s + \frac{btd^2}{2}E_s + \frac{bc^3}{12}E_c \qquad (2)$$

$$EI_{(edge)} = \frac{tb^3}{6}E_s + \frac{cb^3}{12}E_c \qquad (3)$$

3.1.2 Core shear failure

In the flatwise position, shear failure occurs when the shear strength of the core is exceeded while shear failure in the edgewise position occur when the shear strength of the skin is exceeded. The peak core shear strength P_{cs} for specimen in the flatwise direction is predicted by equation 4 and in the edgewise direction using equation 5:

$$P_{cs(flat)} = \frac{2\tau_c D}{(E_s td/2 + E_c c^2/8)} \qquad (4)$$

$$P_{CS(edge)} = \frac{4\tau_s b(2t + cE_c/E_s)}{3} \qquad (5)$$

where: τ_c = shear strength of the core

τ_s = shear strength of the skin

E_c = modulus of elasticity of core

In addition, the peak strength due to core shear failure is estimated using the shear modulus of the skin and the core. This relationship is considered as the modulus of elasticity of the core is only 1/13 to that of the modulus of elasticity of the skin, however, its shear modulus is almost 3/10 to that of the skin. The peak strength P_{csG} for sandwich beams in the flatwise position is predicted using equation 6 and in the edgewise position using equation 7. In equation 6, *GI* is

calculated similarly as equations 2 and 3 with the modulus of elasticity of the skin and the core replaced with its corresponding shear modulus.

$$P_{csG(flat)} = \frac{2\tau_c GI}{(G_s td/2 + G_c c^2/8)} \quad (6)$$

$$P_{csG(edge)} = \frac{4\tau_s b(2t + {}^{cG_c}\!/_{G_s})}{3} \quad (7)$$

where: G_s = shear modulus of the skin

G_c = shear modulus of the core

3.1.3 Core failure in tension and compression

Similarly, the core will fail if the normal stress in tension and/or compression is exceeded. Since the tensile strength of the modified phenolic core material is less compared to its compressive strength, it is predicted to fail first due to tensile failure. The peak strength P_{cf} in the flatwise and edgewise directions for this failure mode can be predicted by:

$$P_{cf(flat)} = \frac{D\sigma_c}{CLE_c({}^{c}\!/_{2})} \quad (8)$$

$$P_{cf(edge)} = \frac{D\sigma_c}{CLE_c({}^{b}\!/_{2})} \quad (9)$$

where: σ_c = maximum bending strength of the core

3.2 Stress-strain relationship of composite sandwich beams

A simple Fibre Model Analysis or FMA [25] was conducted to determine the stress-strain relationship of the top and bottom skins of the composite sandwich beams in the flatwise and edgewise positions. The model was based on the layer-by-layer approach to evaluate the sectional forces corresponding to a given strain distribution at a specific section. Nominal flexural capacity was calculated from the constitutive behaviours of the fibre composite skin and

the core using strain compatibility and force equilibrium principles. A perfect bond exists between the skin and the core, and the strains in the skins and the core were assumed directly proportional to the distance from the neutral axis. These assumptions were based on Bernoulli's hypothesis of strain compatibility: that plane sections remain plane which require perfect bonding between the fibre composite skins and the core material, and that no slip occurs. Similarly, a perfect bond is assumed between plies of the fibre composite skin. The stresses were computed by multiplying the strain to the modulus of elasticity of the materials and the cross-sectional force equilibrium (in summation of forces, the net tensile force shall be equal to the net compressive force) was applied. The fibre composite skin was assumed to behave linearly elastic until failure. On the other hand, the bilinear elastic behaviour of the core material in compression was used. After cracking of the core, its tensile contribution was neglected.

3.3 Load-deflection behaviour of composite sandwich beams

The load deflection behaviour of the composite sandwich beams was obtained using the shear deformation theory proposed by Timoshenko in 1921 [26]. In the Timoshenko beam theory, the total deflection is the sum of the deflections due to bending and shear deformations. Equations 10 and 11 give the calculated deflection at midspan in a simply supported composite sandwich beam under 4-point bending.

$$\Delta_{4FSW-I} = \frac{23PL^3}{1296D} + \frac{PL}{6AG} \qquad (10)$$

$$\Delta_{4FSW-II} = \frac{59PL^3}{3000D} + \frac{PL}{5AG} \qquad (11)$$

where: Δ_{4FSW-I} = deflection at midspan for specimen 4FSW-I

$\Delta_{4FSW-II}$ = deflection at midspan for specimen 4FSW-II

AG = shear stiffness.

The shear stiffness of the composite sandwiches loaded in the flatwise position is approximated using equation 12 with G equal to the shear modulus of the core. In the edgewise position, the core of the composite sandwiches were transformed into an equivalent skin material. A transformation factor n_G, which is defined as the ratio of the shear modulus of the core to that of the skin is introduced. The shear area in the edgewise position is then calculated using equation 13. In this equation, the contribution of the skin in the shear rigidity of the composite sandwich is considered. After cracking of the core, its contribution to the flexural and shear stiffness was neglected.

$$AG_{(flat)} = bdG_c \quad (12)$$

$$AG_{(edge)} = (2t + n_G c)bG_s \quad (13)$$

4. Finite element modelling of composite sandwich beam behaviour

Numerical simulations were carried out to verify the analytical solutions and to compare with the experimental measurements of the flexural behaviour of the composite sandwich beams. The simulations of the 4-point static bending test of the composite sandwich beams have been carried out using Strand7 finite element program [27]. The skin and the core material were modelled as 8-noded layered solid brick elements with mechanical properties obtained from the coupon tests. The brick elements had aspect ratios between 1.1 and 1.4. The FEM model was carried out simulating the specimen and the loading set-up in the actual experimental conditions to have a reliable result. Due to symmetry, only one-fourth of the sandwich beam was modelled to reduce the computational time. Figure 4 shows the numerical model used to simulate the 4-point static bending tests of the composite sandwich beams in the flatwise and in edgewise positions.

Non-linear analyses were conducted considering the combined effect of the linear elastic behaviour of the skin and the non-linear behaviour of the core material and the large displacements of the sandwich beams before final failure. The skin was modelled as linear

elastic orthotropic materials until failure while the core, with linear stress-strain relationship in tension and bi-linear stress-strain relationship in compression. In addition, the skin was assumed to be perfectly bonded to the core, eliminating the delamination failure mode.

5. Experimental results and discussions

The experimental results of the 4-point static bending test of the composite sandwich beams are discussed in the following subsections. The load-displacement relationship, load-strain relationship and the failure mode of specimen in the flatwise and edgewise positions are discussed in detail.

5.1 Load deflection relationship

The typical load displacement relationship of the composite sandwich beams is shown in Figures 5 and 6. Figure 5 shows that the load capacity of specimen 4FSW-I-F increased linearly with deflection until a load of 3000 N. A slight decrease in stiffness was observed after this load due to crack initiation in the core material. When the core failed, an abrupt drop in the load was observed and the specimen failed subsequently (point A). The specimen 4FSW-I-F failed at an applied load of around 4650 N with a midspan deflection of 13.7 mm.

The load-deflection behaviour of specimen 4FSW-I-E showed linear behaviour but a slight reduction in stiffness was observed with the appearance of damage. At a load of around 6,700 N (point B), tensile cracking in the core was observed at the constant moment region. At this stage, the strain gauge attached to the tensile side of the specimen broke and could no longer measure the strain. At a maximum applied load of 8,150 N (point C), a significant drop in load was observed due to the compressive failure of the skin followed by shearing of the core. After the load drop, the specimen continued to sustain load but never exceeded the previous peak load as only the fibre composite skins were carrying the load. The specimen then failed due to the tensile failure of the fibre composite skin.

Figure 6 shows the load and midspan deflection relation of specimens 4FSW-II-F and 4FSW-II-E. The specimen 4FSW-II-F failed at an applied load of around 4880 N with a midspan deflection of 25.6 mm (point E). The load of specimen 4FSW-II-E increased linearly with deflection but showed a reduction in stiffness at a load of around 4000 N and a deflection of 6.9 mm (point F). The specimen then continued to carry load until compressive failure of the skin at a load of 5250 N and a deflection of 10.6 mm (point G). A significant drop in load was observed but the specimen continued to carry load until tensile failure of the fibre composite skin (point H).

In general, the composite sandwich beams in the flatwise position deflected more than twice the specimen in the edgewise position under the same level of applied load. This is due to the increase in the moment of inertia of specimen in the edgewise position as deflection is inversely proportional to the effective moment of inertia. The composite sandwich beams in the edgewise position failed at a higher load than that of the flatwise position. The presence of the non-horizontal skins in the edgewise position prevented the premature failure of the core material and resulted to ductile behaviour.

5.2 Stress-strain relationship

Figure 7 shows the typical bending stress and bending strain relationship at the top and bottom surface of the composite sandwich beams in the flatwise and the edgewise directions. The stresses at the top and bottom skins were determined by transposing equation 1. The tensile and compressive strains on the other hand were determined from the strain gauges attached to the specimen. The tensile stress-strain relation is designated with (T) while the compressive stress-strain relation is designated with (C).

The results suggest that the strains in both tension and compression increased linearly with stress for all specimens before any failure was observed. A slight decrease in stiffness at a strain of around 6,000 micro strain was observed due to the initiation of core cracking at the tensile

side of the specimen. The specimen 4FSW-I-F failed at a stress of around 147 MPa and tensile strain of 10,300 micro strain. These stress and strain levels were only 60% of the maximum stress and strain of the fibre composite skins established from the test of coupons. This premature failure of specimen 4FSW-I-F occurred due to the combine flexure and shear as this specimen has relatively shorter span. At a stress of around 170 MPa and a strain of 12,000 micro strains, the strain gauge at the tension side of specimen 4FSW-I-E broke indicating the developments of flexural cracks. The specimen 4FSW-I-E failed at a compressive stress of 205 MPa and a compressive strain of around 12,800 micro strains.

Both specimens 4FSW-II-F and 4FSW-II-E reached the maximum stress of 201 MPa and strain of 12400 micro strains. These values represent the stress and strain at which the fibre composite skins failed in compression based from the results of the coupon tests. The specimen 4FSW-II-F failed at a compressive stress of around 213 MPa and strain of 13,300 micro strains while the specimen 4FSW-II-E failed at a compressive stress of around 226 MPa and strain of 16500 micro strains. The slightly higher values of failure stress and strain of specimen 4FSW-II-E could be due to the presence of a thicker core which prevented the compression buckling of the fibre composite skins thereby, slightly delaying its failure.

5.3 Failure mode

Figures 8 and 9 show the typical failure mode of the composite sandwich beams. The results of the experiment showed that the specimen 4FSW-I-F failed in a brittle manner due to failure of the core under the loading point followed by the propagation of shear cracks toward the edges of the specimens (Figure 8a). This observed failure could be due to the combined effect of shear and flexural stresses as these specimens have relatively shorter span than specimen 4FSW-II. One of the specimens tested failed due to local skin wrinkling (Figure 8a). A close observation on the specimen revealed that this failure occurred due to the presence of voids on the compressive skin.Tensile cracks in the core was observed at the constant moment region of

specimen 4FSW-I-E. However, the non-horizontal skins prevented the crack width from increasing and did not cause failure. The specimens continued to carry load until compressive failure of the fibre composite skins (Figure 8b).

Figure 9a shows that the specimen 4FSW-II-F failed due to compressive failure of the fibre composite skin followed by the successive debonding between the compressive skin and the core. Tensile cracking of the core was observed in specimen 4FSW-II-E. However, the presence of the non-horizontal skins prevented the crack width from increasing to cause failure. The specimen 4FSW-II-E failed in a ductile failure mode due to the progressive compressive failure of the fibre composite skin followed by tensile failure of the skin (Figure 9b).

6. Predicted results and comparison with experiments

The results of the analytical prediction and numerical simulations of the flexural behaviour of the composite sandwiches and comparison with the experimental results are discussed in the succeeding sections.

6.1 Failure load

Simple beam theory using the effective mechanical properties of the glass fibre skins and the core was used to determine the maximum load and the governing failure for the composite sandwich beams. Table 4 shows the predicted failure load and the maximum load of the composite sandwiches based on experimental investigations. The results showed that the predicted failure load of specimen 4FSW-I-F using equations 4 and 6 are 40% and 25% higher than the actual failure load, respectively. This shows that using the shear modulus of the skin and the core can better predict the failure load of the composite sandwich beams due to core shear failure. The difference however on the predicted and the actual failure load could be due to the combine effect of flexural stresses which resulted in a slightly lower failure load.

The predicted failure load due to tensile failure of the core is lower than that of the actual failure load for specimen 4FSW-I-E as the specimen failed due to compressive failure of the skin. The predicted load due to the compressive failure of the skin is nearly equal (1.5% lower) to that of the actual failure load. This shows that the failure of the composite sandwich beam in the edgewise position occurred only when the fibre composite skin failed in compression.

The predicted load due to tensile failure of the core for specimen 4FSW-II-F is 5% lower than the actual. However, the predicted load due to compressive failure of the skin is only 3% lower. This clearly showed that for longer specimens under bending, the failure load of the composite sandwich beams is governed by failure of the fibre composite skins. For specimen 4FSW-II-E, the predicted load due to compressive failure of the skin is comparable to the actual failure load. Similar to the specimen 4FSW-I-E, the non-horizontal skins of specimen 4FSW-I-E prevented the core shear failure and failure occurred only when the fibre composite skin failed in compression.

6.2 Stress-strain relationship of composite sandwich

The stress-strain relationship of the fibre composite skins predicted analytically and numerically and the result of the 4-point bending tests on composite sandwiches are shown in Figures 10 and 11. In these figures, the experimental, FEM and the FMA stress-strain relation are designated by Expt, FEM and FMA, respectively.

The experimental results show an almost linear stress-strain relationship in both tension and compression and a good agreement with the predicted stress-strain relation based on the FMA and FEM. A higher strain is measured in the tension than in compression which further confirms that the fibre composite skins have a slightly lower modulus in tension than in compression as observed in the test of coupons. The strain at the top of the sandwich beams matches the strain at the bottom. This showed that the assumption of compatibility of strains throughout the depth of the section, and the equilibrium of internal force resultants is valid. In all specimens, a slight

decrease in stiffness was observed at a tensile strain of 6,000 micro strains. This is due to the initiation of tensile cracking of the modified phenolic core material. Furthermore, the recorded maximum compressive strain of 13,000 micro strains is comparable with the failure strain of fibre composite skin in compression.

In general, results showed that both FMA and FEM analysis can predict the stress-strain behaviour of composite sandwiches. The difference in the FMA and the experimental results is less than 5%. The small discrepancy observed could be attributed to the variations in the dimensions of the composite sandwich specimens.

6.3 Load-deflection relationship of composite sandwich

The comparison of the analytical, numerical and experimental load and midspan deflection curves for composite sandwich beams tested under 4-point static bending are shown in Figures 12 to 15. Using the constitutive material behaviour of the fibre composite skin and the phenolic core determined from the coupon tests, the analytical and the numerical models have provided results in good agreement with the experiment.

Figures 12 and 14 show that the difference in the predicted and the experimental results is only 2% for composite sandwich beams tested in the flatwise position. However, the difference between the predicted and experimental results can go as high as 5% for specimen in the edgewise position. The reason for this could be due to the behaviour of the non-horizontal skin as it is subjected both to flexural and shear deformation. Similarly, the skins are subjected both to tension and compression not unlike in the flatwise position wherein the fibre composite skins is subjected only to either compressive or tensile forces.

Figures 13 and 15 show the comparison of the experimental and analytical prediction considering and not considering shear deformation. The analytical load-deflection behaviour of the composite sandwich beams in the flatwise and edgewise position which does not include shear deformation are designated as FMA-F(2) and FMA-E(2), respectively. The shear

deflection of specimen 4FSW-I loaded in the flatwise position is around 5% of the total deflection and around 8% in the edgewise position (Figure 13). However, the contribution of shear in the total deflection decreased for specimen 4FSW-II due to the longer test spans. The shear deformation of specimen in the flatwise position is only 3% and only 6% in the edgewise position (Figure 15). The higher shear deflection in the edgewise position is due to the contribution of the non-horizontal skins in the shear rigidity of the sandwich beams.

6.4 Failure mode

The failure mechanisms of the composite sandwiches under 4-point static bending based on the numerical simulations is shown in Figure 16 and 17. The result of the FEM analysis showed a good agreement with the experimental results as well as the predicted failure mode using analytical formula for composite sandwich beams. Using the maximum stresses where the skin and the core will fail, the FEM analysis was successful in the prediction of the failure mechanisms of the composite sandwiches tested in flatwise and in edgewise positions. Based on the FEM model, the shear failure of the core under the loading point of the specimen 4FSW-I tested in the flatwise position (Figure 16a) occurred at a load of 4650 N while compressive failure of the composite skin in the edgewise position (Figure 16b) occurred at a load of 8000 N. On the other hand, specimen 4FSW-II will both failed due to compressive failure of the skin. Compressive failure of the skins occurred at a load of 4500 N for specimen tested in the flatwise position and a load of 5500 N for specimen in the edgewise position (Figure 17). In all specimens, the failure mechanisms predicted from the FEM simulations are similar to the failure mechanisms observed in the experimental investigation. These results further shows that using the material properties determined from the coupon tests, the numerical models have provided results in good agreement with the experiment.

7. Conclusions

The flexural behaviour and failure mechanisms of an innovative composite sandwich beams in flatwise and edgewise positions have been studied experimentally, analytically and numerically. The experimental investigation showed that under flexural loading, the composite sandwich beams in the flatwise position failed with sudden brittle type failure. In the edgewise position, the presence of fibre composite skins increased the ultimate strength of the composite sandwiches. When tensile cracks of the core occurred, the non-horizontal skins prevented it from widening and prevented the sudden failure of the composite sandwich.

The contribution of the high strength core material in the flexural and shear stiffness is significant and should be included to determine the overall behaviour of the composite sandwiches. Theoretical prediction of failure loads using the mechanical properties of the constituent materials established from the coupon tests was found to be in good agreement with the experimental results. In the simple FMA and FEM simulations, consideration of the bilinear elastic behaviour of the core material in compression provided a better understanding of the flexural behaviour of composite sandwiches.

Finally, the result of this study showed the high potential of this innovative composite sandwich material for structural laminated beam. An increase in flexural stiffness due to sandwich effect suggest the application of composite sandwich beams in flatwise position in the outermost layers to carry tensile and compressive stresses. Similarly, the higher capacity of the composite sandwich beams in the edgewise position suggest that the strength is significantly improved by the introduction of the non-horizontal fibre composite skins, thus could be used in the inner portion of the laminated beams to carry shear. However, the behaviour of a number of these fibre composite sandwich beams bonded together should be investigated further to pave the way in the development of structural components from this composite material.

Acknowledgements

The authors are very grateful to Dr. Gerard Van Erp of LOC Composites, Pty. Ltd. for providing the fibre composite sandwiches and for his valuable suggestions in conducting this study.

References

[1] American Society of Testing and Materials. ASTM standard terminology of structural sandwich constructions (C274-99). West Conshohocken, PA: ASTM International 1999.

[2] Belouettar, S, Abbadi, A, Azari, Z, Belouettar, R, Freres, P. Experimental investigation of static and fatigue behaviour of composite honeycomb materials using four point bending tests. Composite Structures 2008; 87(3), pp 265-273.

[3] Russo, A, Zuccarello, B. Experimental and numerical evaluation of the mechanical behaviour of GFRP sandwich panels. Composite Structures 2007; 81, pp 575-586.

[4] Keller, T. Material tailored use of FRP composites in bridge and building construction, Swiss Federal Institute of Technology Lausanne, Switzerland, 2006.

[5] Canning, L, Hollaway, L, Thorne, AM. Manufacture, testing and numerical analysis of an innovative polymer composite/concrete structural unit', Proceedings of Inst. Civil Engineering Structures and Buildings 1999; 134, pp 231-241.

[6] Humpreys, MF, Van Erp, GM, Tranberg, C. The structural behaviour of monocoque fibre composite truss joints. Advanced Composite Letters 1999; 8(4), pp173-180.

[7] Omar, T. Multi-pultrusion fibre composite truss systems for deployable shelters, PhD dissertation, University of Southern Queensland, Toowoomba, Queensland, Australia, 2008.

[8] Hollaway, LC & Head, PR. Advanced polymer composites and polymers in the civil infrastructure. Elsevier Science Ltd., Oxford, UK, 2001.

[9] Davalos, JF, Qiao, PZ, Xu, XF, Robinson, J, Barth, KE. Modelling and characterization of fibre-reinforced plastic honeycomb sandwich panels for highway bridge applications. Journal of Composite Structures 2001; 52, pp 441-452.

[10] Rocca, SV, Nanni, A. Mechanical characterization of sandwich structure comprised of glass fibre reinforced core: Part I. Composites in Construction 2005 – Third International Conference, Lyon, France.

[11] Daniel, IM, Abot, JL. Fabrication, testing and analysis of composite sandwich beams. Composites Science and Technology 2000; 60, pp. 2455-2463.

[12] Dai, J, Thomas Hahn, H. Flexural behaviour of sandwich beams fabricated by vacuum-assisted resin transfer moulding. Composite Structures 2003; 61, pp 247-253.

[13] Wicks, N, Hutchinson, JW. Optimal truss plates. International Journal of Solids and Structures 2001; 38, pp. 5165-5183.

[14] Shenhar, Y, Frostig, Y, Altus, E. Stresses and failure patters in the bending of sandwich beams with transversely flexible cores and laminated composite skins. Composite Structures 1996; 35, pp. 143-152.

[15] Kampner, M, Grenestedt, JL. On using corrugated skins to carry shear in sandwich beams. Composite Structures 2007; 85, pp. 139-148.

[16] Van Erp, G, Rogers, D. A highly sustainable fibre composite building panel. Proceedings of the International Workshop on Fibre Composites in Civil Infrastructure – Past, Present and Future, 1-2 December 2008, University of Southern Queensland, Toowoomba, Queensland, Australia.

[17] Mouritz, AP, Thomson, RS. Compression, flexure and shear properties of a sandwich composite containing defects. Composite Structures 1999; 44, pp. 263-278.

[18] Jen, Y-M, Chang, L-Y. Evaluating bending fatigue strength of aluminium honeycomb sandwich beams using local parameters. International Journal of Fatigue 2008; 30, pp 1103-1114.

[19] Reis, EM, Rizkalla, SH. Material characteristics of 3-D FRP sandwich panels. Construction and Building Materials 2008; 22, pp. 1009-1018.

[20] Bootle, KR. Wood in Australia. Types, properties and uses. Mc-Graw Hill Book Company, Sydney, 1983.

[21] ASTM C 393 – 00. Standard test method for flexural properties of sandwich constructions. 1916 Race St., Philadelphia, Pa 19103.

[22] Steeves, CA, Fleck, NA. Collapse of sandwich beams with composite face sheets and a polymer foam core: experiment versus theory. International Journal of mechanical Science, 2004.

[23] Vinson, JR. The behaviour of sandwich structures of isotropic and composite materials. Technomic, Lancaster, Pa, 1999.

[24] Bekuit, JRB, Oguamanam, DCD, Damisa, O. A quasi-2D finite element formulation for the analysis of sandwich beams. Finite Elements in Analysis and Design 2007; 43, pp 1099-1107.

[25] Park, R, Paulay, T. Reinforced concrete structures. John Wiley and Sons Ltd, 1975.

[26] Bank, LC. Composites for construction: Structural design with FRP materials. John Wiley and Sons, Inc., New Jersey, 2006.

[27] Strand7 Finite Element Analysis System. Sydney, Australia, 2005.

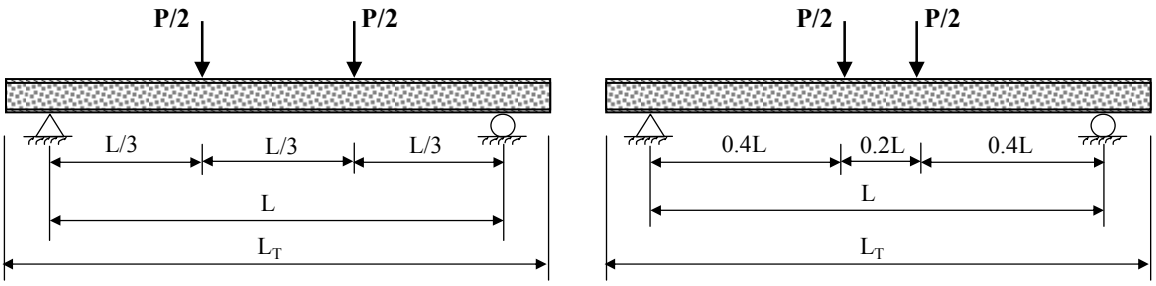

(a) 4FSW-I (b) 4FSW-II

Fig. 1. Schematic illustration of flexural test of composite sandwich

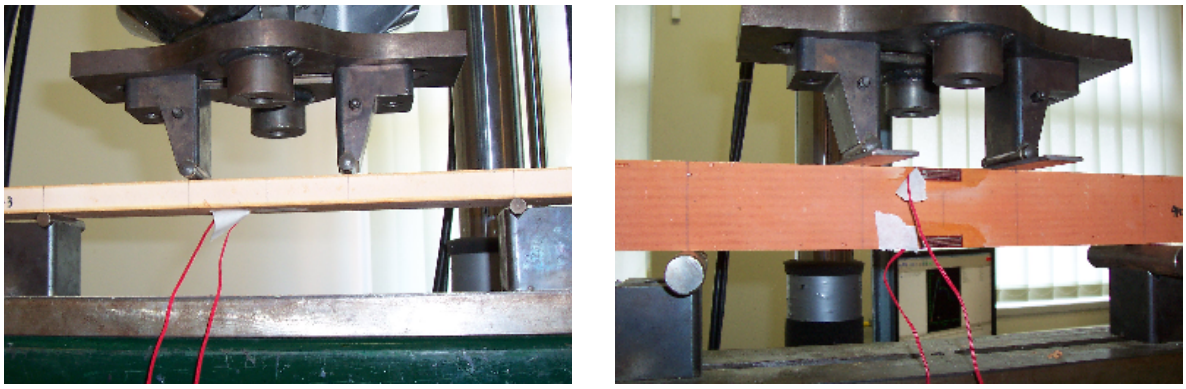

(a) flatwise (b) edgewise

Fig. 2. Test set-up for specimen 4FSW-II

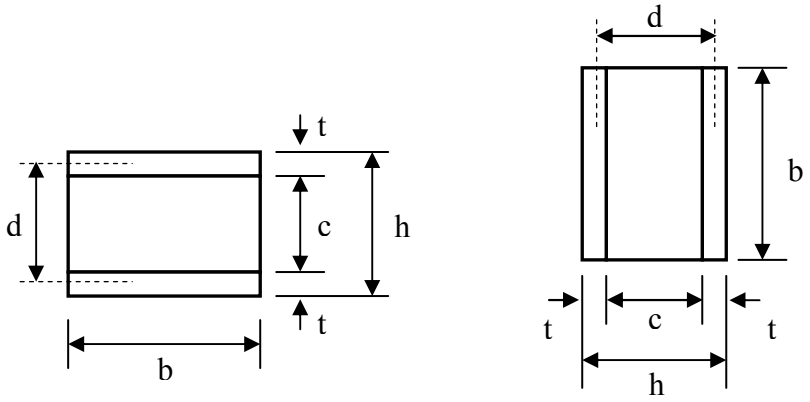

(a) flatwise (b) edgewise

Fig. 3. Composite sandwich section

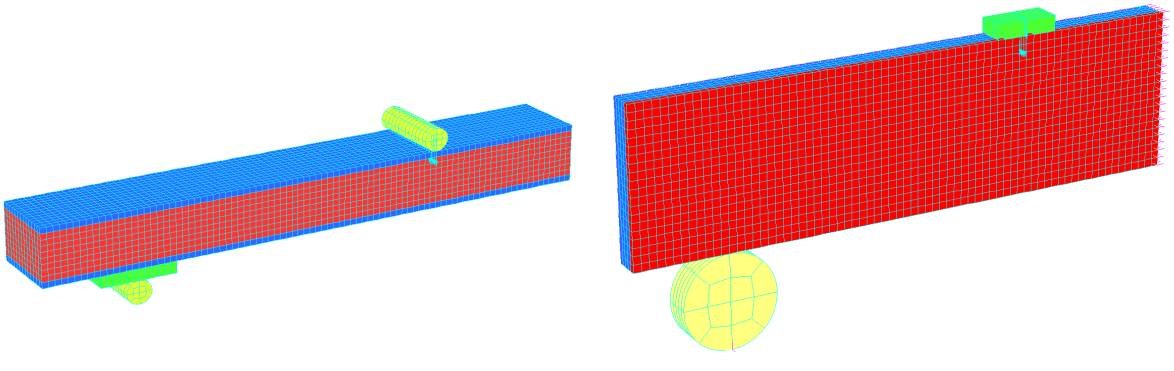

(a) flatwise (b) flatwise

Fig. 4. FEM model of composite sandwiches under 4-point bending

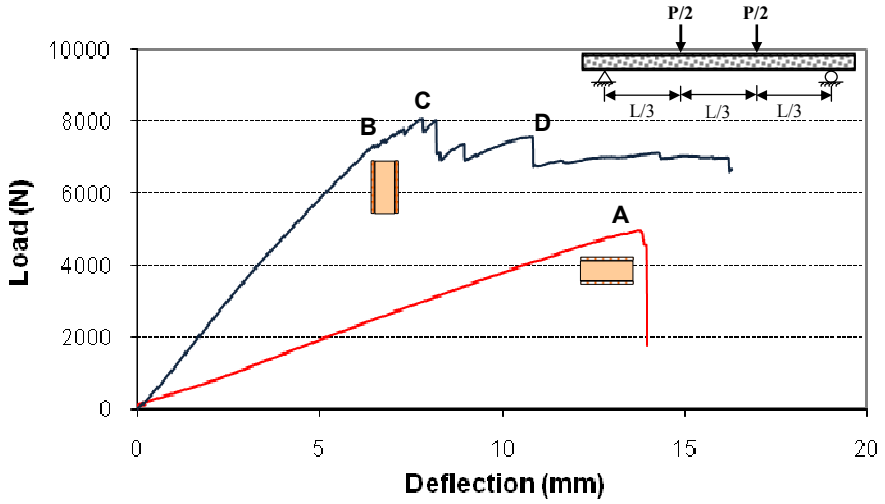

Fig. 5. Load-midspan deflection relation of specimen 4FSW-I

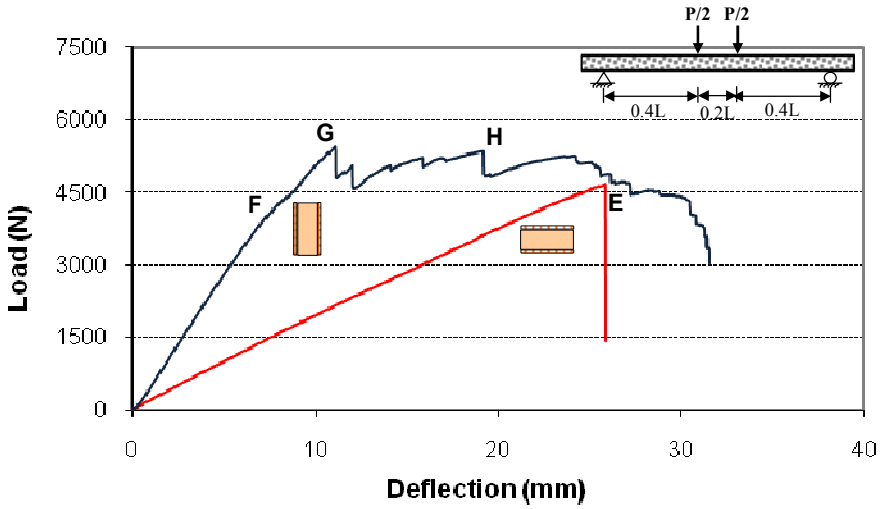

Fig. 6. Load-midspan deflection relation of specimen 4FSW-II

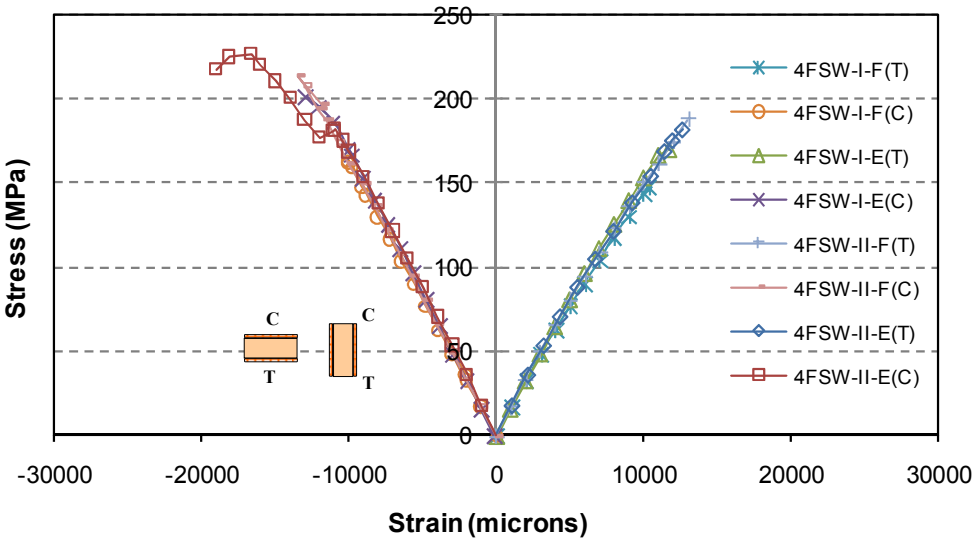

Fig. 7. Stress-strain behaviour of composite sandwiches under 4-point bending

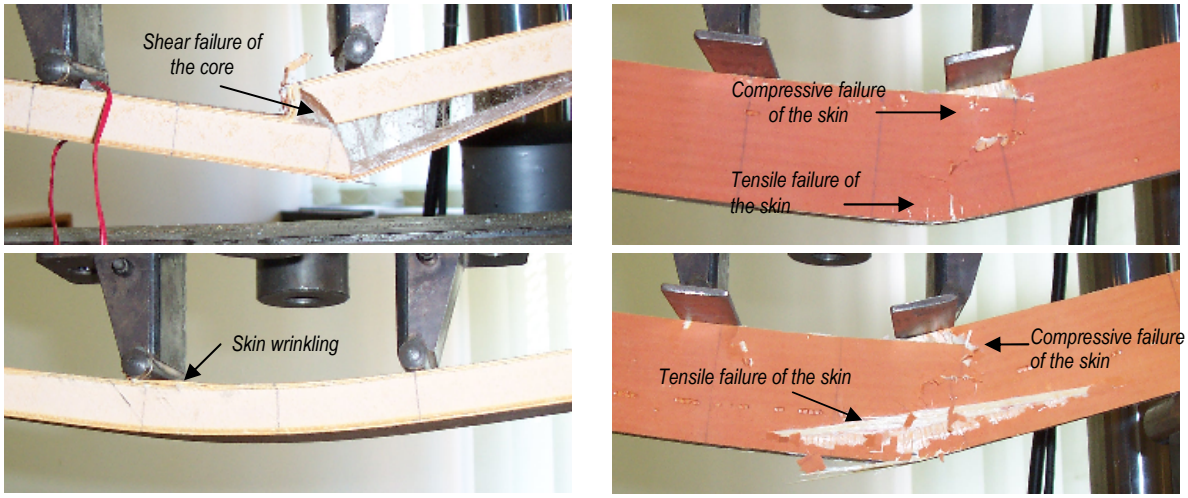

(a) flatwise (b) edgewise

Fig. 8. Failure mode of specimen 4FSW-I

(a) flatwise (b) edgewise

Fig. 9. Failure mode of specimen 4FSW-II

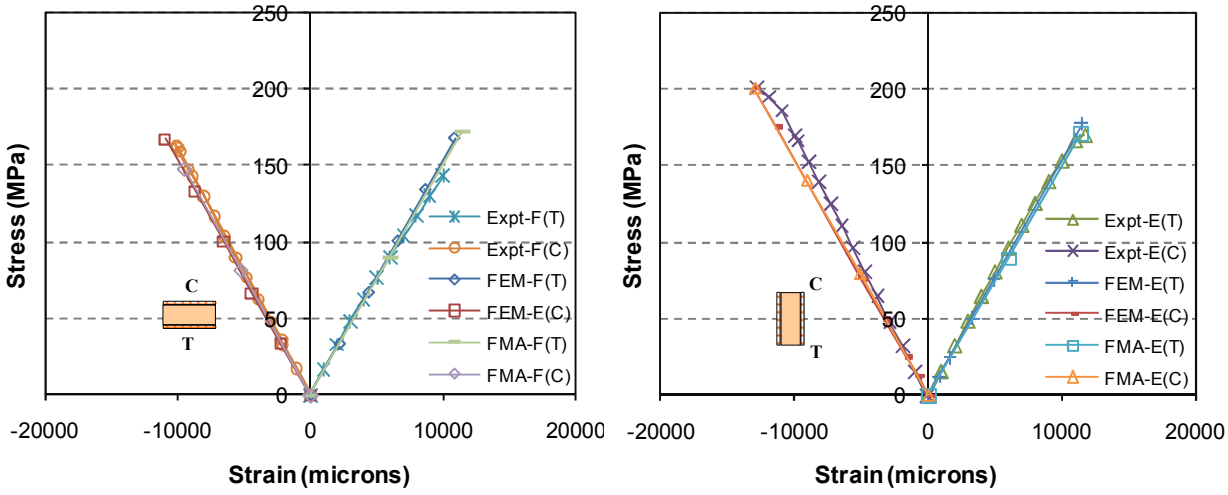

(a) flatwise (b) edgewise

Fig. 10. Analytical, numerical and experimental stress-strain behaviour of specimen 4FSW-I

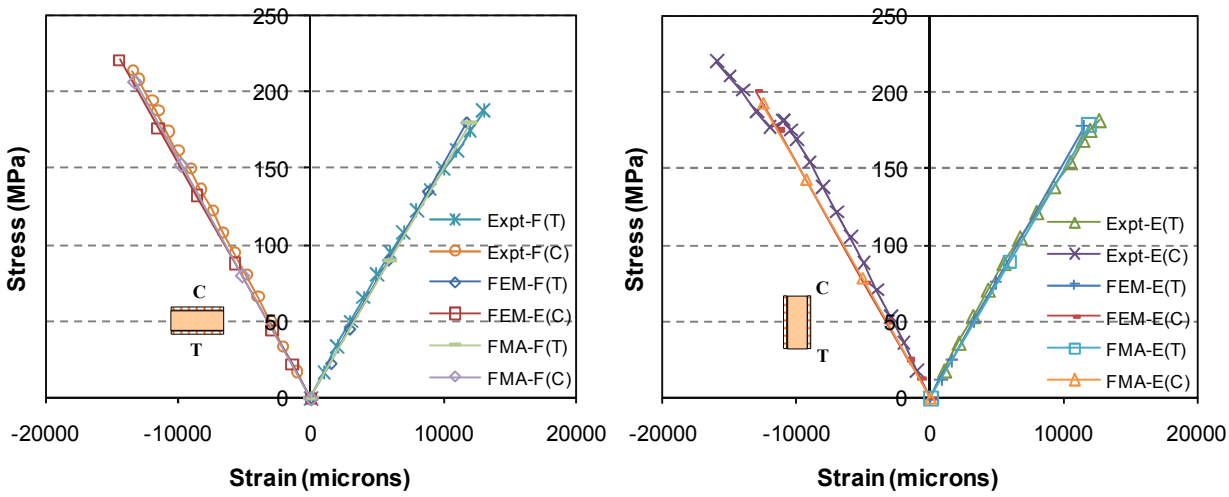

(a) flatwise (b) edgewise

Fig. 11. Analytical, numerical and experimental stress-strain behaviour of specimen 4FSW-II

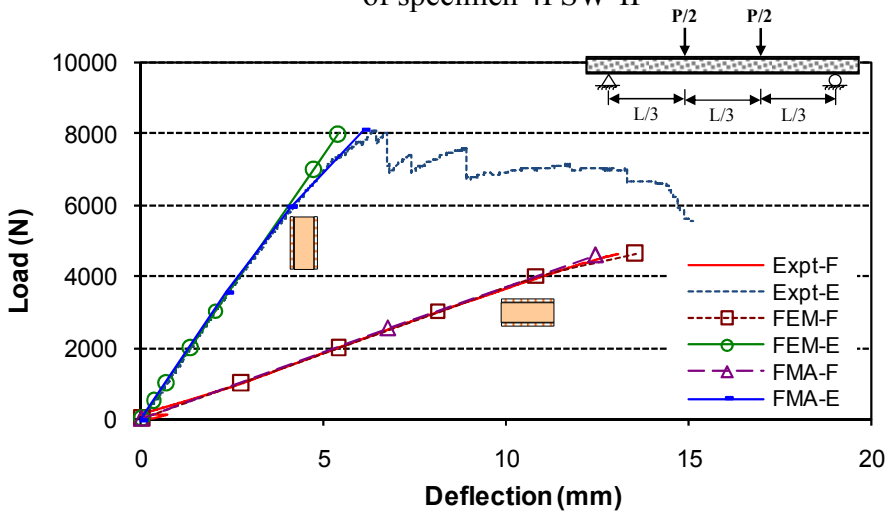

Fig. 12. Analytical, numerical and experimental load-deflection behaviour of specimen 4FSW-I

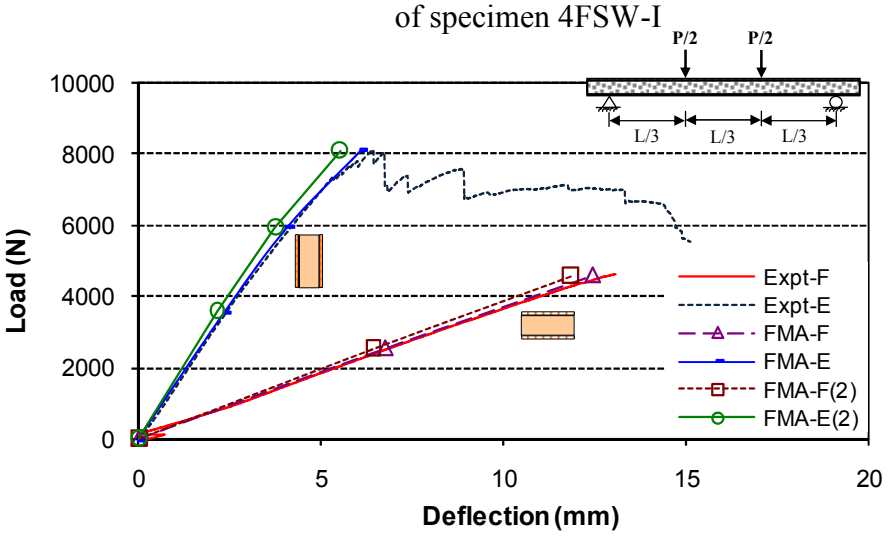

Fig. 13. Load-deflection behaviour of specimen 4FSW-I with and without shear deformation

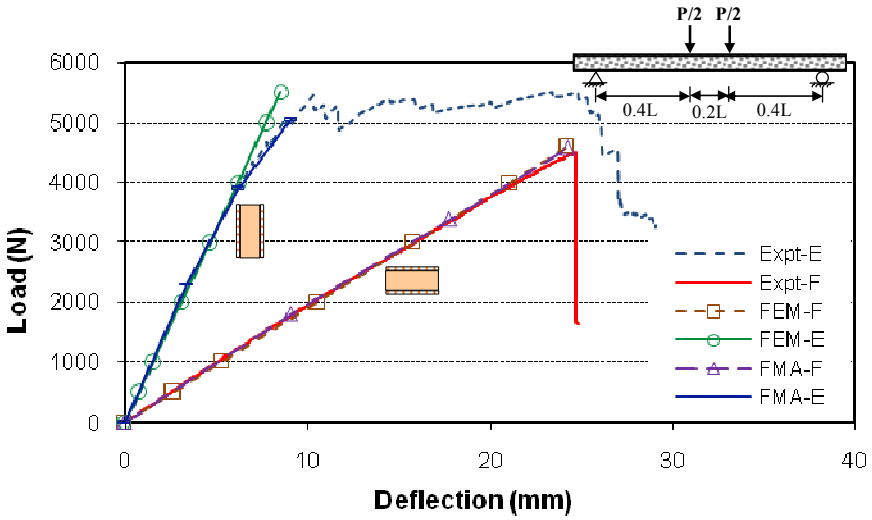

Fig. 14. Analytical, numerical and experimental load-deflection behaviour of specimen 4FSW-II

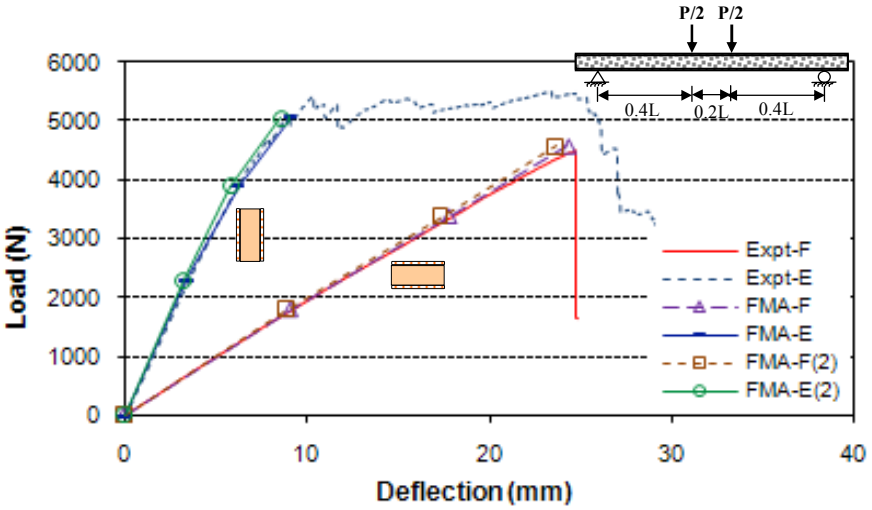

Fig. 15. Load-deflection behaviour of specimen 4FSW-II with and without shear deformation

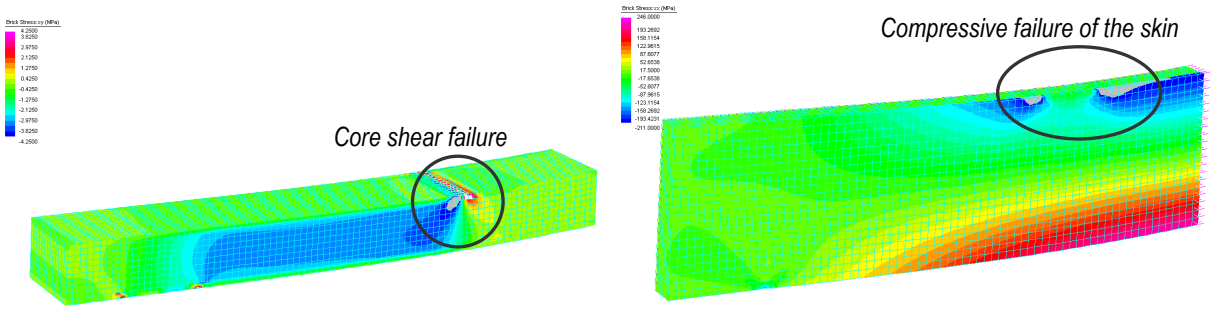

(a) flatwise (b) edgewise

Fig. 16. Predicted failure of specimen 4FSW-I based on FEM analysis

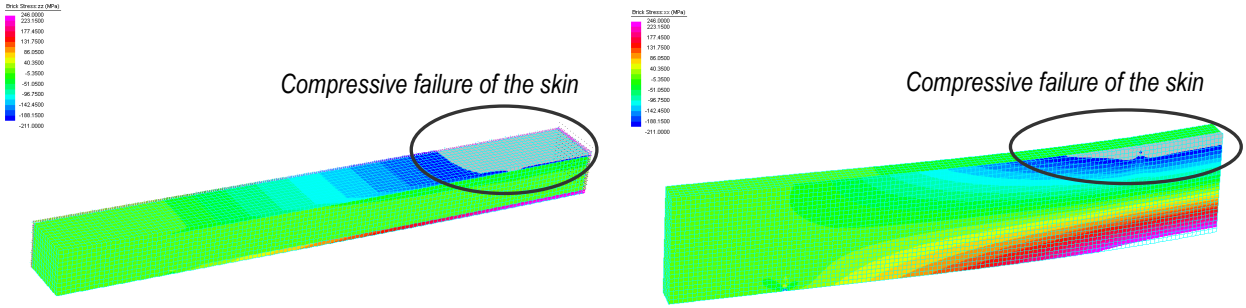

(a) flatwise (b) edgewise

Fig. 17. Predicted failure of specimen 4FSW-II based on FEM analysis

Table 1. Characteristics of the bi-axial glass fibre skins

Property	Longitudinal (0^o) Testing Values		Transverse (90^o) Testing Values	
	Average	Std Dev	Average	Std Dev
Flexural modulus (MPa)	14,284.50	876.02	3,663.98	236.54
Peak stress (MPa)	317.37	27.95	135.05	11.01
Strain at peak (%)	2.29	0.14	5.26	0.43
Tensile modulus (MPa)	15,380.31	745.09	12,631.40	617.99
Peak stress (MPa)	246.80	10.38	208.27	13.26
Strain at peak (%)	1.60	0.01	1.57	0.09
Compressive modulus (MPa)	16,102.39	2,570.40	9,948.61	761.44
Peak stress (MPa)	201.75	28.56	124.23	9.12
Strain at peak (%)	1.24	0.15	1.25	0.06
Shear modulus (MPa)	2,465.82	105.30	2,173.92	171.60
Peak stress (MPa)	22.82	0.69	21.81	0.86
Strain at peak (%)	3.11	0.11	2.38	0.05

Table 2. Characteristics of the modified phenolic core

Property	Testing Values	
	Average	Std Dev
Flexural modulus (MPa)	1,154.40	13.02
Peak stress (MPa)	14.32	0.40
Strain at peak (%)	1.22	0.05
Tensile modulus (MPa)	980.15	55.14
Peak stress (MPa)	5.95	0.31
Strain at peak (%)	0.61	0.02
Compressive modulus (MPa)	2,571.43	99.71
Peak stress (MPa)	21.35	1.13
Strain at peak (%)	1.94	0.07
Shear modulus (MPa)	746.88	4.97
Peak stress (MPa)	4.25	0.19
Strain at peak (%)	0.57	0.03

Table 3. Details of composite sandwich specimens for flexural test

Specimen name	Width, mm	Depth, mm	span, mm	Shear span, mm	Orientation of testing
4FSW-I-F	50	18	300	100	flatwise
4FSW-I-E	18	50	300	100	edgewise
4FSW-II-F	50	20	400	160	flatwise
4FSW-II-E	20	50	400	160	edgewise

Table 4. Actual and predicted failure load of composite sandwiches

Specimen name	Failure load based on experiment, N	Predicted failure load, N			
		[a]Shear failure of core	[b]Shear failure of core	Compressive failure of the skin	Tensile failure of the core
4FSW-I-F	4657	6441	5792	5927	6212
4FSW-I-E	8150	16387	11815	8024	6738
4FSW-II-F	4534	7128	6380	4406	4316
4FSW-II-E	5567	17063	12678	5403	4453

[a]Calculated using equations 4 and 5 for flatwise and edgewise positions respectively.
[b]Calculated using equations 6 and 7 for flatwise and edgewise positions respectively